Quantum Topol. 15 (2024), 503–536
DOI 10.4171/QT/209

α-induction for bi-unitary connections

Yasuyuki Kawahigashi

Abstract. The tensor functor called α-induction produces a new unitary fusion category from a Frobenius algebra object, or a Q-system, in a braided unitary fusion category. In the operator algebraic language, it gives extensions of endomorphism of N to M arising from a subfactor $N \subset M$ of finite index and finite depth, which gives a braided fusion category of endomorphisms of N. It is also understood in terms of Ocneanu's graphical calculus. We study this α-induction for bi-unitary connections, which provides a characterization of finite-dimensional nondegenerate commuting squares, and present certain 4-tensors appearing in recent studies of 2-dimensional topological order. We show that the resulting α-induced bi-unitary connections are flat if we start with a commutative Frobenius algebra, or a local Q-system. Examples related to chiral conformal field theory and the Dynkin diagrams are presented.

1. Introduction

A fusion category [13] has recently emerged as a new type of symmetry in a wide range of topics in mathematics and physics. Theory of operator algebras gives a nice framework to study this type of new symmetries, as exemplified by discovery of the Jones polynomial for knots [24] from the Jones theory of subfactors [23]. We have three operator algebraic realizations of a fusion category based on endomorphisms of a type III factor [37, 38], bimodules over type II_1 factors [15, Chapter 9], and bi-unitary connections [1, Section 3]. The last approach based on bi-unitary connections recently has renewed interest because of its relations to 2-dimensional statistical physics [9, 29].

A certain 4-tensor, a (finite) family of complex numbers indexed by four indices, is studied in physics literature, such as [9, 41]. This has been identified with a bi-unitary connection in the subfactor sense in [29], and further studies [30–32] have followed in this direction. Also, see [20] for a recent development. Bi-unitary connections and related topics are also recently studied in [10, 11]. This approach to a fusion category based on bi-unitary connections has advantage that everything is described with

Mathematics Subject Classification 2020: 46L37 (primary); 18M15, 18M20, 81T40 (secondary).
Keywords: subfactor, modular tensor category, α-induction, bi-unitary connection.

finite-dimensional matrices and thus in principle computable on computers, while endomorphisms of a type III factor and bimodules over type II_1 factors are infinite dimensional. This computability is one reason why physicists are interested in this approach recently. Our aim in this paper to study *α-induction* in this framework of bi-unitary connections.

The tensor functor α-induction originates in the operator algebraic studies of *chiral conformal field theory* [40]. In this context, our basic object is a *conformal net*, which is a family of von Neumann algebras parametrized by intervals contained in the circle S^1. It has a representation theory of *superselection sectors* and this has a structure of *braiding* [16,17]. If a conformal net has a certain finiteness property called *complete rationality*, we obtain a *modular tensor category* of its representations [34]. See a short review [28] and a longer review [27] for a general theory of this topic.

In a classical representation theory, if we have a representation of a subgroup $H \subset G$, we have a method of *induction* to obtain a representation of G. We have a similar, but more subtle, induction machinery for representation theory of conformal nets, depending on braiding structure. Suppose we have an inclusion $A \subset B$ of completely rational conformal nets and λ is a representation of A given as a Doplicher–Haag–Roberts endomorphism of $A(I)$ for some fixed interval I in S^1. Then, we can extend this endomorphism to $B(I)$ using the braiding. This was first defined by Longo–Rehren [40] and further studied by Xu [51] and Böckenhauer–Evans [4–6], where this was named as *α-induction*.

In a completely different setting, Ocneanu had a machinery of *flat connections* to study subfactors [43, 44], which consists of entries of a large unitary matrix. Then, using a braiding structure of flat connections on the Dynkin diagrams of type A, he introduced a graphical calculus to construct new fusion categories related to the Goodman-de la Harpe subfactors [18] in [45]. We have unified the two theories of α-induction and Ocneanu's graphical calculus in a fully general setting of braided fusion categories and proved various basic properties such as appearance of modular invariants in [7, 8] in the framework of endomorphisms of type III factors. In this setting, α-induction is understood as a method of extending an endomorphism of a factor N to another factor $M \supset N$ using braiding, where we do not assume anything about conformal field theory. This α-induction has been also understood in the language of bimodules and more abstract braided fusion category.

Our motivation for this paper is as follows. First, it is nice to have a concrete realization of α-induction in the setting of bi-unitary connections due to its finite dimensionality and relations to statistical physics. Secondly, it gives a generalization of Ocneanu's graphical calculus in a much more general setting. We also note that the same mathematical structure as α-induction appears in the context of anyon condensation [2], which gives another reason to study α-induction in this setting. (See [36, Table 1] for this direction.)

Our main result is Theorem 3.6 which shows our bi-unitary connection defined in Definition 3.5 is a correct description of α-induction. We have a remark that though we use an endomorphism framework [7, 8], we only need abstract properties of α-induction, so we can also use a bimodule framework or a setting based on more abstract fusion categories for α-induction for our results.

2. Preliminaries on braided fusion categories, subfactors, and α-induction

We give our setting for α-induction for a subfactor $N \subset M$ and endomorphisms of N as in [7]. Let N be a type III factor. Throughout this paper, we assume the following for Δ which is a finite set of mutually inequivalent irreducible endomorphisms of N of finite dimension. (See [7, Definition 2.1].)

Assumption 2.1. We have the following for Δ.

(1) The identity automorphism is in Δ.

(2) For any $\lambda \in \Delta$, we have another element $\mu \in \Delta$ which is equivalent to $\bar{\lambda}$.

(3) For any $\lambda, \mu \in \Delta$, the composition $\lambda\mu$ decomposes into a direct sum of irreducible endomorphisms each of which is equivalent to one in Δ.

(4) The set Δ has a *braiding* $\varepsilon(\lambda, \mu) \in \mathrm{Hom}(\lambda\mu, \mu\lambda)$ as in [7, Definition 2.2].

We further make an assumption on connectedness of certain bipartite graphs as follows, which will be necessary in the following Section. Note that this assumption depends on a choice of μ, an irreducible endomorphism of N in Δ. This is assumed throughout the paper, except for Section 6.

Assumption 2.2. Consider a bipartite graph defined as follows. Let both even and odd vertex sets be labeled with the elements in Δ. The number of edges between the even vertex ν_1 and the odd vertex ν_2 is given by $\dim \mathrm{Hom}(\nu_1\mu, \nu_2)$. We assume that this graph is connected.

Endomorphisms of N with finite dimension whose irreducible decompositions give endomorphisms equivalent to ones in Δ produce a fusion category where objects are such endomorphisms and morphisms are intertwiners between endomorphisms. (See [7, Section 2.1] for more details on intertwiners. Also, see [3] for a recent treatment of fusion categories and subfactors. See [13] for a more abstract and algebraic treatment of fusion categories.) We consider a subfactor $N \subset M$ with finite index whose canonical endomorphism θ decomposes into a sum of endomorphisms equivalent to ones in Δ. Such a subfactor automatically has a finite depth. For a fixed N and a fusion category of such endomorphisms, an extension M of N is in a bijective

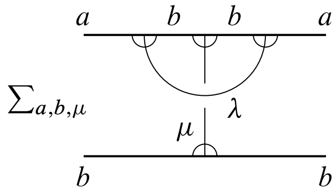

Figure 1. The chiral generator p_λ^+.

correspondence to a *Q-system* as in [39, Section 6]. In algebraic literature, this is often called a *Frobenius algebra*. (In this paper, we only consider C^*-tensor categories. Also, see [42, Theorem 2.3] for a bimodule formulation of a Q-system.)

Since we assume to have a braiding, our fusion category is a braided fusion category. If a braiding is nondegenerate in the sense of [7, Definition 2.3], we say that this braided fusion category is a *modular tensor category*, but we do *not* assume this nondegeneracy in this paper. We have a notion of *locality*, $\varepsilon(\theta,\theta)\gamma(v)=\gamma(v)$, for a Q-system corresponding to a subfactor $N\subset M$. (Here, γ is the canonical endomorphism of M and an isometry $v\in M$ satisfies $vx=\gamma(x)v$ for $x\in M$ and $M=Nv$.) The name "locality" comes from the locality of an extension of a conformal net in the setting of [40, Theorem 4.9], and it was called *chiral locality* in [7]. A local Q-system is also called a *commutative Frobenius algebra* in algebraic literature. We deal with *both* local and non-local Q-systems in this paper.

The procedure called *α-induction* was defined in [40, Proposition 3.9] as follows:

$$\alpha_\lambda^\pm=\bar\iota^{-1}\cdot\mathrm{Ad}(\varepsilon^\pm(\lambda,\theta))\cdot\lambda\cdot\bar\iota,$$

where λ is an endomorphism in Δ, ι is the inclusion map $N\hookrightarrow M$, $\theta=\bar\iota\cdot\iota$ is the dual canonical endomorphism of $N\subset M$, and $\pm$ stands for a choice of positive/negative braiding. It is a nontrivial fact that $\mathrm{Ad}(\varepsilon^\pm(\lambda,\theta))\cdot\lambda\cdot\bar\iota(x)$ is in the image of $\bar\iota$ for $x\in M$. We have $\alpha_\lambda^\pm(x)=\lambda(x)$ for $x\in N$ and $\alpha_\lambda^\pm(v)=\varepsilon^\pm(\lambda,\theta)^*v$. See [7, Section 3] for basic properties of α-induction in this setting.

In a very different setting, Ocneanu used Figure 1 to represent a chiral generator in the double triangle algebra. (Also, see [7, Figure 47].) It was identified with the α-induction in [7, Theorem 5.3]. (See [7, Section 4] for the double triangle algebra and [7, Figure 4.1] for a graphical convention involving small half circles.)

For various diagrams, we use the convention in [7, Section 3]. In particular, our convention is as in Figure 2, where T is an isometry in $\mathrm{Hom}(\lambda,\mu\nu)$ as in [7, Figure 21]. Note that rotation invariance of this type of diagrams is due to the *Frobenius reciprocity* for endomorphisms due to Izumi [21, 22]. Also, as in [7, Section 4], we draw a thin wire for an N-N morphism, a thick wire for an N-M or M-N morphism,

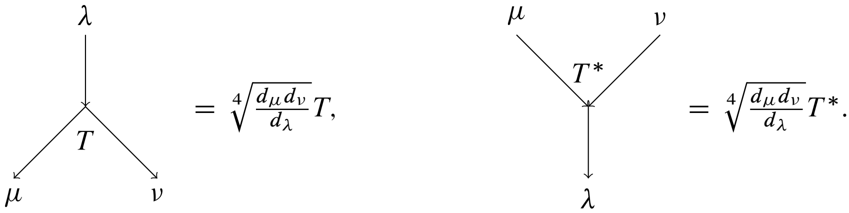

Figure 2. Graphical convention for normalization of an intertwiner.

and a very thick wire for an M-M morphism. For a thick wire, we can tell whether it stands for an N-M or M-N morphism from a diagram.

3. α-induction for bi-unitary connections

We now produce a family of new bi-unitary connections from the setting as in the previous section. We simply say a connection for a bi-unitary connection in this paper.

We first recall the definition of a connection. (See [15, Section 11.3], [1, Section 3], and [32, Section 2]. There is an issue of connectedness of certain graphs and we follow conventions of [1, Section 3] on this matter.)

We have four finite bipartite graphs $\mathcal{G}, \mathcal{G}', \mathcal{H}, \mathcal{H}'$. The vertex set V_0 is common for even vertices of $\mathcal{G}$ and $\mathcal{H}$. Similarly, the vertex sets V_1, V_2, V_3 are common for odd vertices of $\mathcal{H}$ and $\mathcal{G}'$, even vertices of $\mathcal{G}'$ and $\mathcal{H}'$, and odd vertices of $\mathcal{G}$ and $\mathcal{H}'$, respectively. The four graphs satisfy some properties about the Perron–Frobenius eigenvalues and eigenvectors as in [32, Section 2]. We choose edge $\xi_0, \xi_1, \xi_2, \xi_3$ from the graphs $\mathcal{H}, \mathcal{G}', \mathcal{H}', \mathcal{G}$, respectively, so that they make a closed square called a *cell*. A map W called a *connection* assigns a complex number to each of such cells. This complex value is represented with a diagram in Figure 3. This map W satisfies axioms called *bi-unitarity* as in [32, Definition 2.2]. (See also Figures 8, 9, and 10 below.) The name “bi-unitarirty” means that each number in Figure 3 is an entry of a unitary matrix in two ways, one after normalization arising from the Perron–Frobenius eigenvector entries. Now, we require that the graphs $\mathcal{G}$ and $\mathcal{G}'$ to be connected, but we do *not* require this for $\mathcal{H}$ and $\mathcal{H}'$. (This convention is different from the one in [32], and the same as in [1].) We have an equivalence relation for connections on the same four graphs as in remark after [1, Theorem 3]. We call the graphs $\mathcal{G}, \mathcal{G}', \mathcal{H}, \mathcal{H}'$ the horizontal top graph, the horizontal bottom graph, the vertical left graph and the vertical right graph of W, respectively. We also call the vertices in V_0, V_1, V_2, V_3 the upper left vertices, the lower left vertices, the lower right vertices and the upper right vertices, respectively.

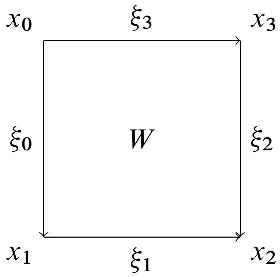

Figure 3. The four graphs for a connection.

It is well known that this bi-unitarity condition is characterized in terms of a *commuting square* as we now explain below. A commuting square of finite-dimensional C^*-algebras

$$\begin{array}{ccc} A & \subset & B \\ \cap & & \cap \\ C & \subset & D \end{array}$$

with a trace on D is characterized by the following mutually equivalent conditions. (See [15, Proposition 9.51], for example.)

(1) The conditional expectation E_B from D to B with respect to trace restricted to C coincides with the conditional expectation E_A from C to A with respect to trace.

(2) The conditional expectation E_C from D to C with respect to trace restricted to B coincides with the conditional expectation E_A from B to A with respect to trace.

This notion was originally considered in [46]. We say that this commuting square is *nondegenerate* if the span BC is equal to D. (Being nondegenerate is also sometimes said to be *symmetric*.) A nondegenerate square of finite dimensional C^*-algebras is described with a connection, for which we do not know yet whether it satisfies bi-unitarity, as in [15, Section 11.2]. Then, it has been proved in [49, Theorem 1.10] that the square gives a commuting square if and only the connection satisfies bi-unitarity. (Also, see [15, Theorem 11.2].) In this sense, having a bi-unitary connection and having a nondegenerate commuting square of finite-dimensional C^*-algebras are the same thing.

A commuting square also naturally appears from a subfactor $N \subset M$ with finite Jones index as

$$\begin{array}{ccc} M' \cap M_k & \subset & M' \cap M_{k+1} \\ \cap & & \cap \\ N' \cap M_k & \subset & N' \cap M_{k+1} \end{array},$$

where $N \subset M \subset M_1 \subset M_2 \subset \cdots$ is the Jones tower arising from the Jones basic construction [23]. (Also, see [15, Section 9.6] for such a commuting square.) If the

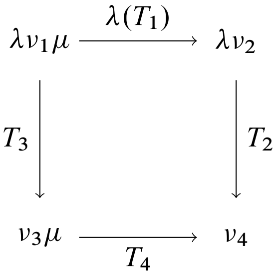

Figure 4. The diagram for the connection $W_1(\lambda, \mu)$ in Figure 5.

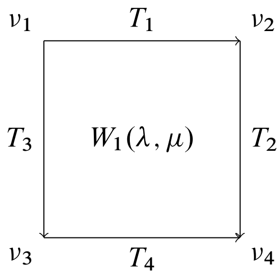

Figure 5. The standard diagram for the connection $W_1(\lambda, \mu)$.

original subfactor $N \subset M$ is hyperfinite, of type II_1 and of *finite depth*, then the above commuting square recovers the original subfactor $N \subset M$ by Popa's theorem [47]. In this sense, a connection encodes complete information about such a subfactor. A connection corresponding to such a commuting square arising from a subfactor $N \subset M$ satisfies a special extra property called *flatness*, which was introduced by Ocneanu [43,44] and studied in [26]. (See [15, Section 11.4] for more discussions on flatness.)

We first define the connection $W_1(\lambda, \mu)$, but we make a remark on one issue again. In this paper, we use operator algebraic realization of a braided fusion category and α-induction based on endomorphisms of a type III factor as in [7,8], such as [7, Figure 30], but this is simply because this was the first place where all necessary details were worked out, and we can equally use other formulations based on bimodules or abstract fusion categories. Such a choice of formulation does not cause any change in our results here.

Definition 3.1. Let $\nu_1, \nu_2, \nu_3, \nu_4 \in \Delta$. Consider the diagram in Figure 4. By composing isometries $T_1 \in \mathrm{Hom}(\nu_1\mu, \nu_2)$, $T_2 \in \mathrm{Hom}(\lambda\nu_2, \nu_4)$, $T_3 \in \mathrm{Hom}(\lambda\nu_1, \nu_3)$, and $T_4 \in \mathrm{Hom}(\nu_3\mu, \nu_4)$, we obtain a complex number $T_4 T_3 \lambda(T_1^*) T_2^* \in \mathrm{Hom}(\nu_4, \nu_4)$. We define the connection $W_1(\lambda, \mu)$ by this number and draw Figure 5.

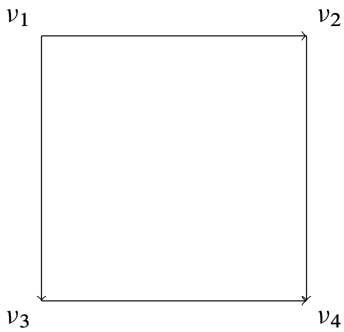

Figure 6. The standard diagram for a connection $W_1(\lambda, \mu)$.

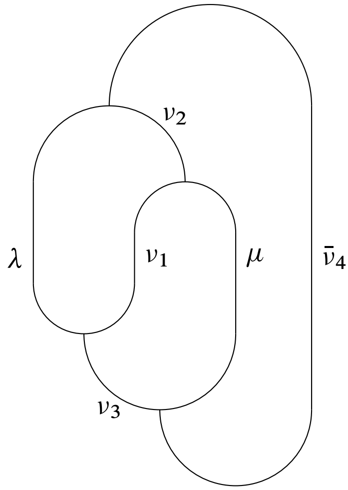

Figure 7. The diagram for the connection $W_1(\lambda, \mu)$ in Figure 5.

We note that the left vertical bipartite graph in this definition is defined as follows. One set of vertices is given by Δ and the other is the same. The number of edges between the vertices ν_1 and ν_3 is given by $\dim \mathrm{Hom}(\lambda\nu_1, \nu_3)$. The other graphs are defined similarly, and this remark applies to all the definitions of the connections in this section.

We often drop labels for the connection and/or intertwiners as long as no confusion arises, and simply draw a diagram in Figure 6.

We draw a diagram as in Figure 7 which represents a complex number in the standard convention as in [7, Section 3]. (Note that in Figure 7, we drop orientations of wires which go from the top to the bottom.) This complex number is equal to the one represented by the composition of isometries as in Figure 4 multiplied by $\sqrt{d_\lambda d_\mu d_{\nu_1} d_{\nu_4}}$ by the standard convention in Figure 2.

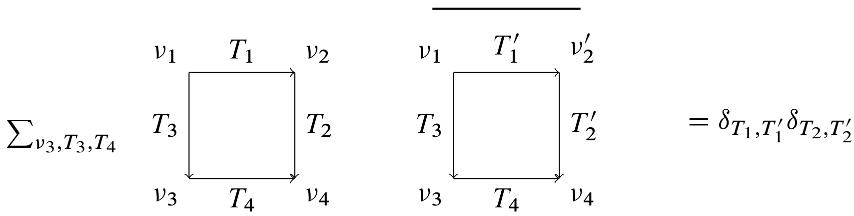

Figure 8. Unitarity (1) for the connection $W_1(\lambda, \mu)$.

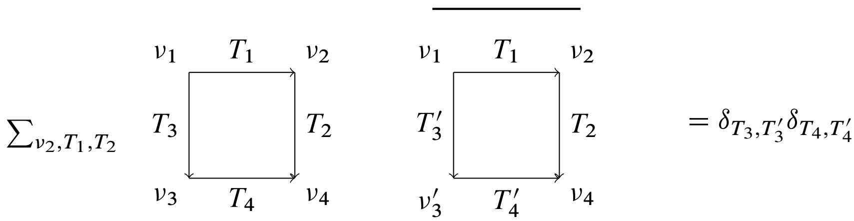

Figure 9. Unitarity (2) for the connection $W_1(\lambda, \mu)$.

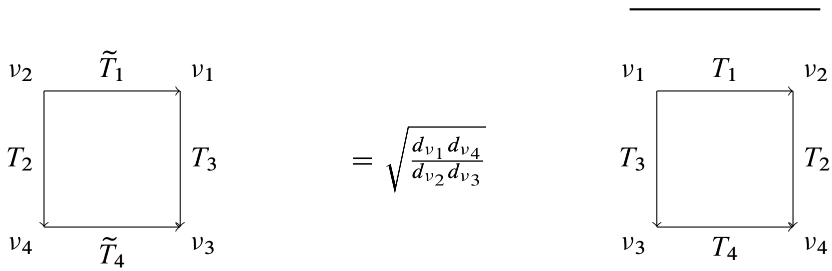

Figure 10. Crossing symmetry for the connection $W_1(\lambda, \mu)$.

Then, unitarity of the connection $W_1(\lambda, \mu)$ is represented as in Figures 8 and 9. Here, the bars above the right squares denote the complex conjugates.

Crossing symmetry for the connection $W_1(\lambda, \mu)$ is given as in Figure 10, where $\widetilde{T}_1$ and $\widetilde{T}_4$ stand for the Frobenius duals of T_1 and T_4, respectively. This is a well-known relation arising from the tetrahedral symmetry of the $6j$-symbols as in [15, Definition 12.15], but we include a simple argument for this, because we need a similar argument later for $W_3(\lambda)$ as in Figure 21.

We first make a vertical reflection of the diagram in Figure 7 to obtain Figure 11. We then redraw Figure 11 to obtain Figure 12, which represents the complex number given by the diagram in Figure 13 multiplied by $\sqrt{d_\lambda d_{\nu_2} d_\mu d_{\nu_3}}$.

This shows we have crossing symmetry, Figure 10. This, together with the unitarity of the left-hand side of Figure 10, shows bi-unitarity of the connection $W_1(\lambda, \mu)$.

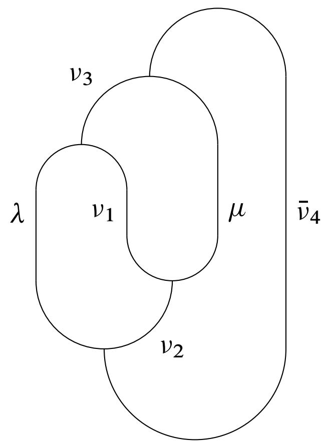

Figure 11. A vertical reflection of Figure 7.

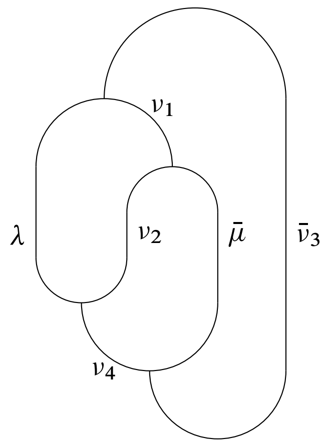

Figure 12. Redrawing of Figure 11.

We now prove that the fusion category of endomorphisms of N arising from Δ and the one arising from the connections $W_1(\lambda, \mu)$ for various λ and fixed μ are equivalent. This is where we need Assumption 2.2. Then, we have the following theorem.

Theorem 3.2. *Under Assumptions 2.1 and 2.2, the fusion category arising from the connections $W_1(\lambda, \mu)$ for all $\lambda \in \Delta$ is equivalent to the one arising from endomorphisms $\lambda \in \Delta$ of N.*

Proof. By the description of the intertwiners between open string bimodules in the proof of [1, Theorem 3], we have a natural injective linear map from $\mathrm{Hom}(\lambda_1\lambda_2, \lambda_3)$

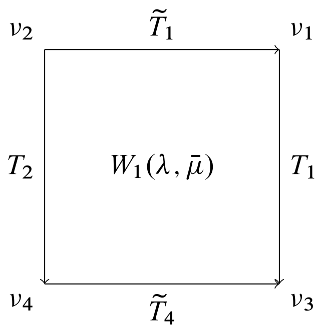

Figure 13. The diagram for the connection $W_1(\lambda, \bar{\mu})$.

to $\mathrm{Hom}(W_1(\lambda_1, \mu)W_1(\lambda_2, \mu), W_1(\lambda_3, \mu))$ for $\lambda_1, \lambda_2, \lambda_3 \in \Delta$. The morphism space $\mathrm{Hom}(W_1(\lambda_1, \mu)W_1(\lambda_2, \mu), W_1(\lambda_3, \mu))$ is described with the higher relative commutants of the corresponding subfactor by the proof of [1, Theorem 3]. These higher relative commutants are described with $C_{k,-1}$ for the subfactor $M_0 \subset M_1$ in the proof of [48, Theorem 3.3]. They are described with the intertwiner spaces of the N-N morphisms as in the proof of [48, Theorem 3.3]. This means that the dimensions of the two intertwiner spaces $\mathrm{Hom}(\lambda_1\lambda_2, \lambda_3)$ and $\mathrm{Hom}(W_1(\lambda_1, \mu)W_1(\lambda_2, \mu), W_1(\lambda_3, \mu))$ are the same, and thus, the above natural linear map is surjective. The compositions of intertwiners in the two fusion categories are also compatible with this identification, so they are equivalent. ■

Then, we see that the structure of the *braided* fusion category of these endomorphisms of N passes to that of these connections.

We next introduce two types of connections. The first is the easier one $W_2(\mu)$.

Definition 3.3. Let $\nu_1, \nu_2 \in \Delta$ and a_1, a_2 be irreducible M-N morphisms arising from Δ and the subfactor $N \subset M$. Figure 14 represents the complex number

$$T_4 T_3 \iota(T_1)^* T_2^* \in \mathrm{Hom}(a_2, a_2)$$

for isometries

$$T_1 \in \mathrm{Hom}(\nu_1\mu, \nu_2), \quad T_2 \in \mathrm{Hom}(\iota\nu_2, a_2),$$
$$T_3 \in \mathrm{Hom}(\iota\nu_1, a_1), \quad T_4 \in \mathrm{Hom}(a_1\nu_2, a_2),$$

where a_1 and a_2 are M-N morphisms. We define the connection $W_2(\mu)$ by this number and use the diagram as in Figure 15 to represent this connection.

Note that remark after Definition 3.1 applies here again. For example, the left vertical bipartite graph in this definition is defined as follows. One set of vertices

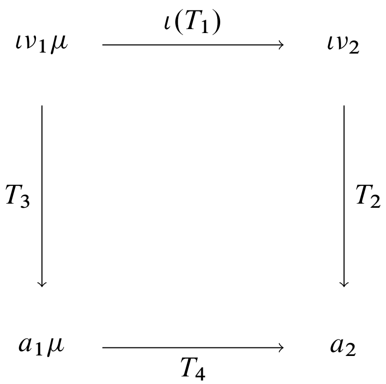

Figure 14. The diagram for the connection $W_2(\mu)$.

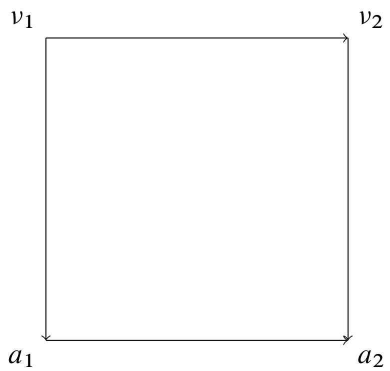

Figure 15. The standard diagram for the connection $W_2(\mu)$.

is given by Δ and the other is given by the representatives of the irreducible M-N morphisms. The number of edges between the vertices $\nu_1 \in \Delta$ and an M-N morphism a_1 is given by $\dim \mathrm{Hom}(\iota\nu_1, a_1)$.

We next introduce the other connection, $W_3(\lambda)$.

Definition 3.4. Let $\nu_1, \nu_2 \in \Delta$ and a_1, a_2 be irreducible M-N morphisms arising from Δ and the subfactor $N \subset M$. Figure 16 represents the complex number

$$T_4\alpha_\lambda^+(T_3)\mathcal{E}^+(\lambda,\iota)^*\iota(T_1)^*T_2^* \in \mathrm{Hom}(a_2, a_2)$$

for isometries $T_1 \in \mathrm{Hom}(\lambda\nu_1, \nu_2)$, $T_2 \in \mathrm{Hom}(\iota\nu_2, \nu_4)$, $T_3 \in \mathrm{Hom}(\iota\nu_1, a_1)$, $T_4 \in \mathrm{Hom}(\alpha_\lambda^+ a_1, a_2)$, which is represented with the connection diagram in Figure 17. We define the connection $W_3(\lambda)$ by this number. Here, $\mathcal{E}^\pm$ is defined in [7, page 455 below equation (14)] and we recall Figure 18, which is taken from [7, Figure 30].

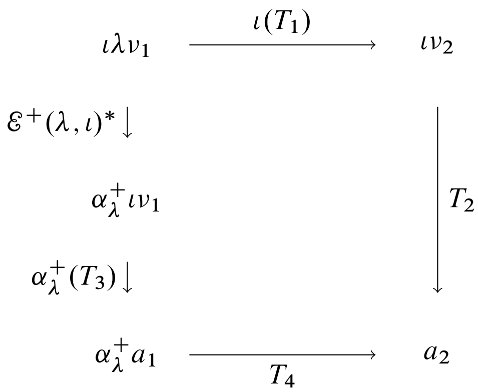

Figure 16. The diagram for the connection $W_3(\lambda)$.

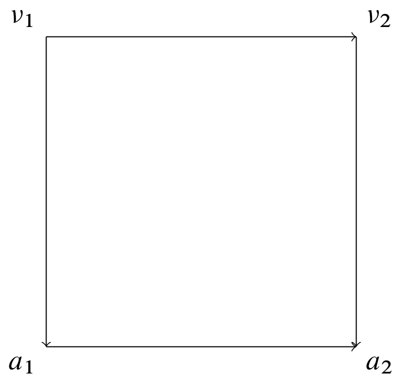

Figure 17. The standard diagram for the connection $W_3(\lambda)$.

The complex number represented by the diagram in Figure 19 is equal to the one represented by the connection diagram in Figure 17 multiplied by $\sqrt{d_\iota d_\lambda d_{\nu_1} d_{a_2}}$ by the standard convention in Figure 2. Note that we drop orientations of wires which go from the top to the bottom in Figure 19.

We make a vertical reflection of Figure 19 to get Figure 20. We again drop orientations of wires which go from the top to the bottom. Note that the complex number values given by these two diagrams are complex conjugate to each other.

By redrawing Figure 20, we have Figure 21.

The complex number represented by the diagram in Figure 21 is equal to the one represented by the connection diagram in Figure 22 multiplied by $\sqrt{d_\lambda d_\iota d_{\nu_2} d_{a_1}}$ This means that the value of the connection diagram in Figure 22 for $W_3(\bar\lambda)$ is equal to the complex conjugate of the value of the connection diagram in Figure 17 for

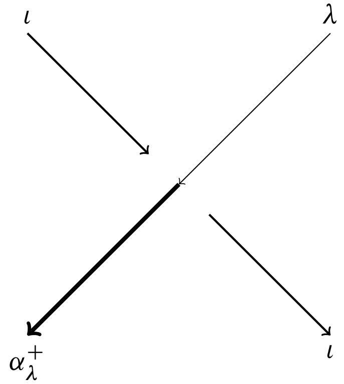

Figure 18. The braiding operator $\mathcal{E}^+(\lambda, \iota)^*$.

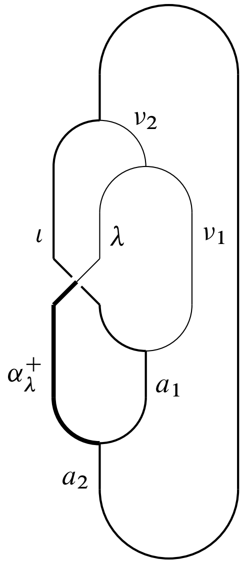

Figure 19. The diagram for the connection $W_3(\lambda)$ in Figure 17.

$W_3(\lambda)$ multiplied by $\sqrt{\frac{d_{\nu_1} d_{a_2}}{d_{\nu_2} d_{a_1}}}$. This proves bi-unitarity of $W_3(\lambda)$, as Figure 10 gave bi-unitarity of $W_1(\lambda, \mu)$.

We next introduce the connection $W_4(\alpha_\lambda^+, \mu)$, which is the α^+-induced connection.

Definition 3.5. Let a_1, a_2, a_3, a_4 be irreducible M-N morphisms arising from Δ and the subfactor $N \subset M$. Consider the diagram in Figure 23. By composing isometries

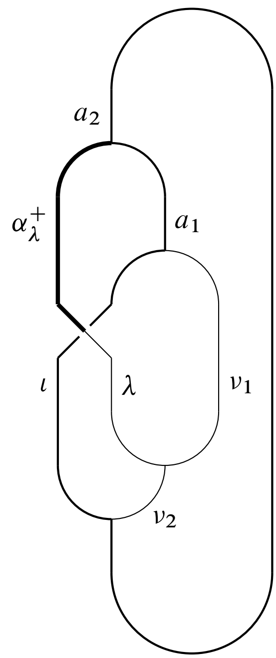

Figure 20. A vertical reflection of Figure 19.

$T_1 \in \mathrm{Hom}(a_1\mu, a_2)$, $T_2 \in \mathrm{Hom}(\alpha_\lambda^+ a_2, a_4)$, $T_3 \in \mathrm{Hom}(\alpha_\lambda^+ a_1, a_3)$, and $T_4 \in \mathrm{Hom}(a_3\mu, a_4)$, we obtain a complex number $T_4 T_3 \alpha_\lambda^+(T_1^*)T_2^* \in \mathrm{Hom}(a_4, a_4)$. We define the connection $W_4(\alpha_\lambda^+, \mu)$ by this number and represent this as in Figure 24.

By a very similar argument to the one for bi-unitarity of $W_1(\lambda, \mu)$, we obtain bi-unitarity of $W_4(\alpha_\lambda^+, \mu)$.

We then have the intertwining Yang–Baxter equation for $W_1(\lambda, \mu)$, $W_3(\lambda)$, $W_3(\mu)$, and $W_4(\alpha_\lambda^+, \mu)$ as in Figure 25, which was given in [25, Axiom 7]. The meaning of this diagram is as follows. On both hand sides of the identity, the six isometries are fixed for the six boundary edges of the hexagons in the same way. The left-hand side means the summation of the product of the three connection values $W_1(\lambda, \mu)$, $W_3(\lambda)$, and $W_2(\mu)$ over all possible choices of the three isometries corresponding to the three internal edges of the hexagon. The right-hand side means the summation of the product of the three connection values $W_3(\lambda)$, $W_2(\mu)$, and $W_4(\alpha_\lambda^+, \mu)$ over all possible choices of the three isometries corresponding to the three internal edges of the hexagon. Both hand sides are equal because they are both equal to the composition of the six (co-)isometries corresponding to the six boundary edges of the hexagons.

We have seen that α-induction applied to $N \subset M$ produces bi-unitary connections. From this construction and the description of intertwiner spaces for connections as in

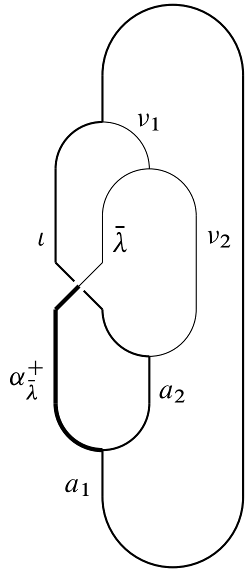

Figure 21. Redrawing of Figure 20.

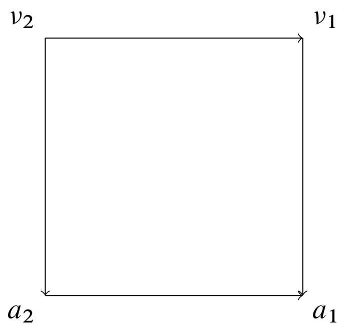

Figure 22. The standard diagram for the connection $W_3(\bar{\lambda})$.

[1, Theorem 3] again, we have the following theorem under Assumption 2.2 with the same arguments as in the proof of Theorem 3.2.

Theorem 3.6. *Under Assumptions 2.1 and 2.2 for a fixed μ, the fusion category arising from the connections $W_4(\alpha^{\pm}_{\lambda}, \mu)$ for all $\lambda \in \Delta$ is equivalent to the one arising from endomorphisms $\alpha^{\pm}_{\lambda}$ of M given by α-induction.*

Note that it is nontrivial that we have only finite many irreducible endomorphisms of M up to equivalence when we consider those arising from $\alpha^{\pm}_{\lambda}$. This has been proved in [7, Theorem 5.10].

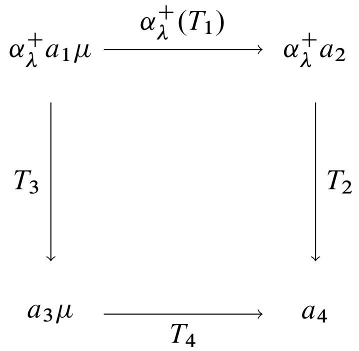

Figure 23. The diagram for the connection $W_4(\alpha_\lambda^+, \mu)$ in Figure 5.

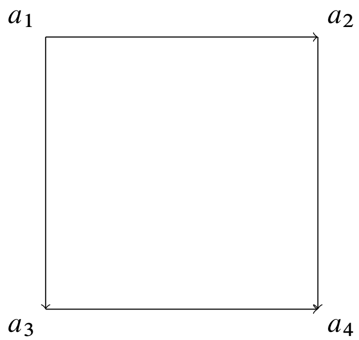

Figure 24. The standard diagram for the connection $W_4(\alpha_\lambda^+, \mu)$.

4. Rewriting $W_4(\alpha_\lambda^+, \mu)$ and switching of positive and negative braiding

Though we have defined the α-induced connection $W_4(\alpha_\lambda^+, \mu)$ as in Figure 23, we need to know full information about α_λ^+ to compute this value. Since we are now in the process of defining the new connection $W_4(\alpha_\lambda^+, \mu)$ before knowing α_λ^+, we certainly hope to compute this number without using the information about α_λ^+. We show in this section that this is possible.

Figure 26 represents the complex number

$$T_4 T_3' \mathcal{E}^+(\lambda, a_1)\alpha_\lambda^+(T_1)^* \mathcal{E}^+(\lambda, a_2)^* T_2'^* \in \mathrm{Hom}(a_4, a_4)$$

for isometries $T_1 \in \mathrm{Hom}(a_1\mu, a_2)$, $T_2' \in \mathrm{Hom}(a_2\lambda, a_4)$, $T_3' \in \mathrm{Hom}(a_1\lambda, a_3)$, $T_4 \in \mathrm{Hom}(a_3\mu, a_4)$, which is represented with the connection diagram in Figure 24. This composition corresponds to the diagram in Figure 27 up to normalization constant,

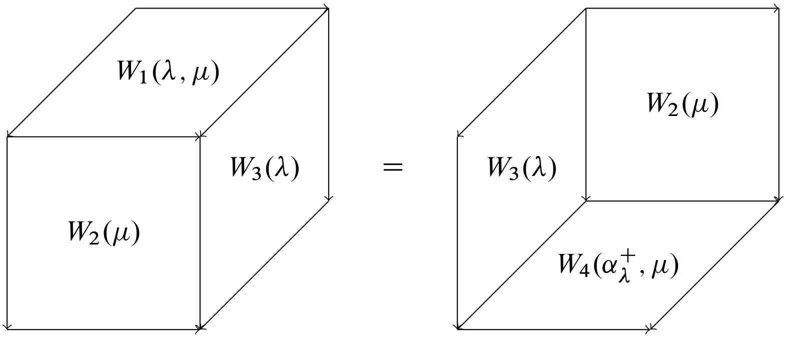

Figure 25. The intertwining Yang–Baxter for $W_1(\lambda,\mu)$, $W_3(\lambda)$, $W_3(\mu)$, and $W_4(\alpha_\lambda^+,\mu)$.

$$\begin{array}{ccc} \alpha_\lambda^+ a_1\mu & \xrightarrow{\alpha_\lambda^+(T_1)} & \alpha_\lambda^+ a_2 \\ \varepsilon^+(\lambda,a_1)\downarrow & & \downarrow\varepsilon^+(\lambda,a_2) \\ a_1\lambda\mu & & a_2\lambda \\ T_3'\downarrow & & \downarrow T_2' \\ a_3\mu & \xrightarrow[T_4]{} & a_4 \end{array}$$

Figure 26. The diagram for the connection $W_4(\alpha_\lambda^+,\mu)$.

and we can redraw this as in Figure 28. Note that we drop orientations of wires which go from the top to the bottom in Figures 27 and 28. The complex number represented by the diagram in Figure 28 is equal to the one represented by the connection diagram in Figure 26 multiplied by $\sqrt{d_\lambda d_\mu d_{a_1} d_{a_4}}$. Since Figure 28 does not involve α_λ^+, this diagram gives $W_4(\alpha_\lambda^+,\mu)$, up to normalization constant, in terms of N-N and M-N morphisms and intertwiners including the braiding operators. This is what we asked for at the beginning of this section.

We next study what the effect of switching the positive and negative braiding is. Vertical reflection of Figure 28 gives Figure 29. The complex numbers given by these two figures are mutually complex conjugate. By comparing these two figures, we have the following proposition.

Proposition 4.1. *We have the identity as in Figure 30.*

We also show that we can rewrite $W_3(\lambda)$ into the form without using α_λ^+ as follows.

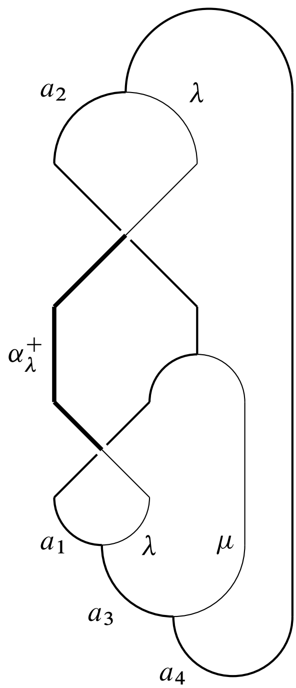

Figure 27. The diagram for the connection in Figure 26.

5. Locality of the Q-system and flatness of $W_4(\alpha_\lambda^+, \mu)$

In the case of Ocneanu's construction [45], he obtained flat connections only for A_n, D_{2n}, E_6, and E_8 as we see in the next section in detail. (Note that Assumption 2.2 does not hold for these examples. We will treat this issue in the following section. Also, see [15, Theorem 11.24].) It has been observed that these cases exactly correspond to the Q-systems with locality $\varepsilon(\theta, \theta)\gamma(v) = \gamma(v)$ as in [8, Section 5] (where this property was called chiral locality). So, we expect some relations between locality of the Q-system and flatness of the corresponding $\alpha^\pm$-induced connection in general. We show that this is indeed the case in this section.

We now assume locality. Note that we then have irreducibility of $\iota : N \hookrightarrow M$ by [4, Corollary 3.6]. (Having a Q-system with locality in a general modular tensor category is enough in [4] rather than a conformal net.)

We prove flatness of the connection $W_4(\alpha_\lambda^+, \mu)$ in the sense of Figure 33, which is taken from [15, Figure 11.21]. We first need a lemma.

Lemma 5.1. *Suppose λ, μ are irreducible endomorphisms of N contained in θ. We then have the identity as in Figure 34.*

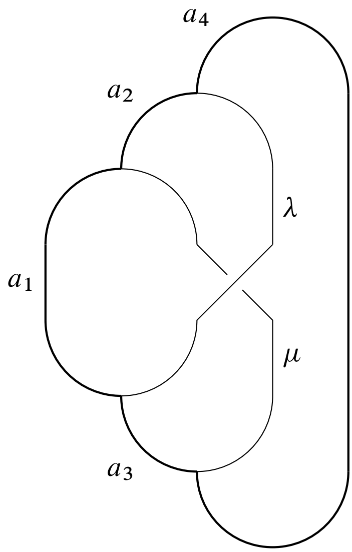

Figure 28. Redrawing of Figure 27.

Proof. Locality gives Figure 35, where the triple vertices on both hand sides represent $\gamma(v)$. We then have the identity in Figure 36, where small black circles represent co-isometries in $\mathrm{Hom}(\theta, \lambda)$ and $\mathrm{Hom}(\theta, \mu)$. We next have the identity in Figure 37 by a property of braiding and then the identity in Figure 38 by rewriting θ with $\bar{\iota}\iota$. Pulling the thick wires straight and rotating this diagram for 90 degrees gives the desired conclusion. ■

Theorem 5.2. *Under Assumption 2.1, the connection $W_4(\alpha_\lambda^+, \mu)$ is flat.*

Proof. We prove the identity in Figure 33. Both horizontal and vertical sizes of the large diagram in Figure 33 are supposed to be even, but we can take both of them to be 1 in our current setting, so we first give a proof for this case.

Now, our $*$ vertex in Figure 33 corresponds to ι. Because all the four corner vertices in Figure 33 are now ι, we set $a_1 = a_2 = a_3 = a_4 = \iota$ in Figure 28. We then have Figure 39 and the complex value this diagram represents is equal to the one given by the partition function in Figure 33 multiplied by $\sqrt{d_\lambda d_\mu} d_\iota$.

By Lemma 5.1, the value Figure 39 represents is equal to the one Figure 40 represents. The latter is equal to $\sqrt{d_\lambda d_\mu} d_\iota$, so the complex value given by the partition function in Figure 33 is 1.

When the horizontal and vertical sizes of the large diagram in Figure 33 are arbitrary, we replace λ and μ in the above arguments by $\bar{\lambda}\lambda \cdots \lambda$ and $\mu\bar{\mu} \cdots \bar{\mu}$. Then, the same arguments give the value 1 and we are done. ■

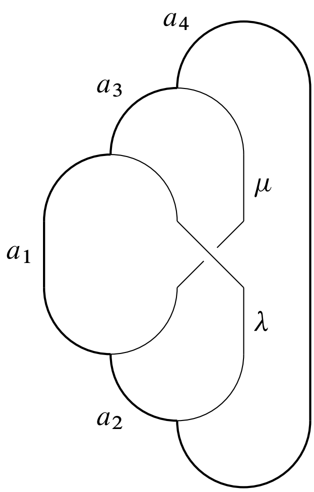

Figure 29. Vertical reflection of Figure 28.

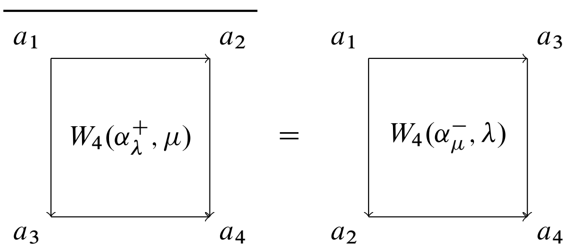

Figure 30. Complex conjugate and opposite braiding.

6. Examples

Ocneanu considered connections on A-D-E Dynkin diagrams in [45]. We revisit this topic from our viewpoint now and would like to apply the results in Section 3. Here, we have a nontrivial issue since Assumption 2.2 does *not* hold now for any choice of μ.

Let Δ be the set of endomorphisms of a type III factor N corresponding to the Wess–Zumino–Witten model $SU(2)_k$, where k is a positive integer called a *level*. (See [12, Subsection 16.2.3], for example.) We label the irreducible objects of the modular tensor category with $0, 1, 2, \dots, k$, using the Dynkin diagram of type A_{k+1} as in Figure 41, where the label 0 denotes the vacuum representation, that is, the identity automorphism of N. Such a system of endomorphisms with braiding has been constructed from a conformal net by Wassermann [50] and this braiding is nondegenerate by [34, Corollary 37] and [52, Theorem 4.1].

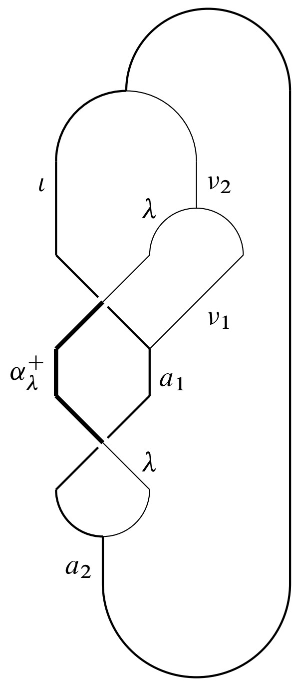

Figure 31. Redrawing of $W_3(\lambda)$.

All Q-systems on Δ for all k have been classified in [33, Section 2.5] for the local case and in [35, Section 2] for the general case. They are classified with a pair consisting of one of the A-D-E Dynkin diagrams and its vertex. We explain this from a viewpoint of the Goodman–de la Harpe–Jones subfactor in [18, Section 4.5].

Let $\mathcal{G}$ be one of the A-D-E Dynkin diagrams and choose the vertex with the smallest entry of the Perron–Frobenius eigenvector entry. We have the Goodman–de la Harpe–Jones subfactor as in [18, Section 4.5] or [15, Section 11.6], and the corresponding Q-system. If $\mathcal{G}$ is of type A, then this Q-system has index 1 and is trivial. If $\mathcal{G}$ is of type D, then the Q-system has index 2 and corresponds to a crossed product by $\mathbb{Z}/2\mathbb{Z}$. If $\mathcal{G}$ is E_6 or E_8, then the Q-systems correspond to the subfactors arising from conformal embeddings $SU(2)_{10} \subset S(5)_1$ and $SU(2)_{28} \subset (\mathrm{G}_2)_1$ by [8, Proposition A.3]. Also, see [8, Appendix] for the case of E_7.

We next choose $\lambda = \mu = 1$ in the setting of Section 3 and consider the connection $W_4(\alpha_\lambda^\pm, \mu)$. Since the irreducible N-M morphisms are labeled with the vertices of $\mathcal{G}$ by the arguments in [15, Section 11.6], all the four vertex sets for $W_4(\alpha_\lambda^\pm, \mu)$ are also labeled with the vertices of $\mathcal{G}$. Then, the requirements for the Perron–Frobenius eigenvalues and the Perron–Frobenius eigenvector entries force all the four graphs of $W_4(\alpha_\lambda^\pm, \mu)$ to be $\mathcal{G}$, but Assumption 2.2 does not hold, since the horizontal top

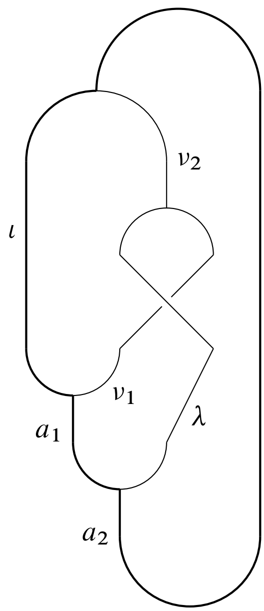

Figure 32. Further redrawing of $W_3(\lambda)$.

and bottom graphs are never connected, due to a $\mathbb{Z}/2\mathbb{Z}$-grading on the vertices of the Dynkin diagrams. This issue is resolved as follows.

The connection $W_4(\alpha_\lambda^\pm, \mu)$ splits into two connections on mutually disjoint graphs both of which are isomorphic to $\mathcal{G}$. Then, both of the two connections must be of the following form as given in [44]. (Also see [15, Figure 11.32].) Let n be its Coxeter number of $\mathcal{G}$ and set $\varepsilon = \sqrt{-1} \exp \frac{\pi\sqrt{-1}}{2(n+1)}$. We write μ_x for the Perron–Frobenius eigenvector entry for a vertex x. Then, our connection is given as follows. (We can replace ε with $\bar{\varepsilon}$. By the arguments in [15, Section 11.5], these two choices give the only possible connections on $\mathcal{G}$. If $\mathcal{G}$ is of type A, they give equivalent connections. If $\mathcal{G}$ is of type D or E, they are not mutually equivalent. Here, we allow only vertical gauges while horizontal gauges are also allowed in [15, Section 11.5], but this does not cause problems since our graph $\mathcal{G}$ is a tree. See remark after [1, Theorem 3].)

The horizontal top and bottom graphs for $W_4(\alpha_j^\pm, 1)$ always have exactly two connected components. This is still valid after we make irreducible decomposition of such connections. Let W be a pair of two such connections W_a and W_b arising from irreducible decomposition of $W_4(\alpha_j^\pm, 1)$ for some j and W' be a pair of two such connections W'_a and W'_b from $W_4(\alpha_k^\pm, 1)$ for some k. We can compose W_a with exactly one of W'_a and W'_b, and compose W_b with the other one, since they have the matching horizontal bottom and top graphs. For the fusion rules and intertwiner spaces of this composition product, we can use either of the two compositions and

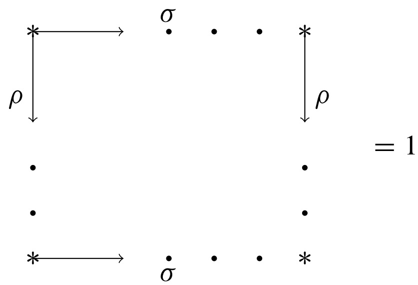

Figure 33. Flatness as in [15, Figure 11.21].

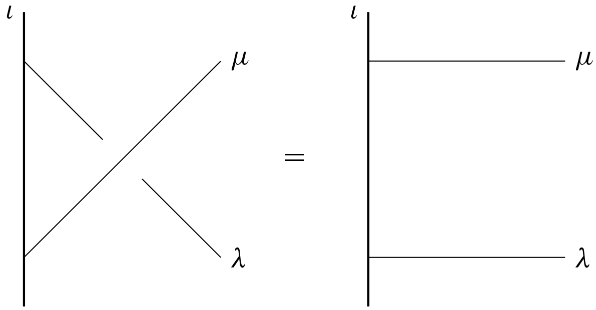

Figure 34. A consequence of locality.

have the same results, by the same arguments as the ones in the proof of Theorem 3.6. In this way, we obtain a fusion category of connections which is equivalent to the one of M-M morphisms arising from $\alpha^{\pm}$-induction. We now obtain the diagrams of decompositions of connections which are the same as in [6, Figures 2, 5, 8, and 9] and [8, Figures 40 and 42]. These were originally found by Ocneanu for such connections. We also know that the results in the previous section on flatness apply to these cases, though Assumption 2.2 does not hold now. For this type of computations, we do not need exact information of the connections, and simply having the graphs involved is often sufficient. See [19] for such computations.

We now discuss the issue of complex conjugate connections. For $W_4(\alpha_1^{\pm}, 1)$, the connection Figure 42 is symmetric in j and m, so the effect of switching positive and negative braiding in Proposition 4.1 now amounts to taking simply complex conjugate connections. That is, $W_4(\alpha_1^+, 1)$ and $W_4(\alpha_1^-, 1)$ are mutually complex conjugate. Now, consider the case of $\mathscr{G} = E_6$. The connections $W_4(\alpha_2^+, 1)$ and $W_4(\alpha_2^-, 1)$ are also mutually complex conjugate. Both of the connections $W_4(\alpha_3^+, 1)$ and $W_4(\alpha_3^-, 1)$ decompose into two irreducible connections each. Since irreducible decomposition of a complex conjugate connection gives the complex conjugate connections of those

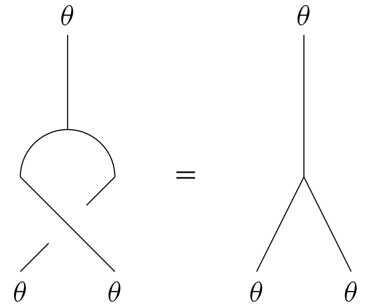

Figure 35. Locality of a Q-system.

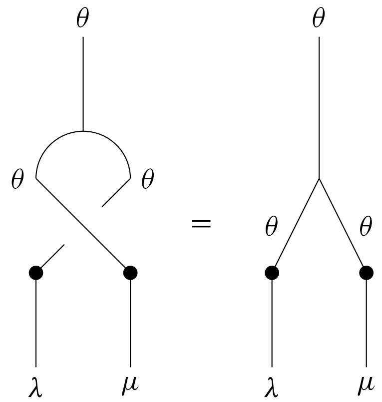

Figure 36. A consequence of Figure 35.

appearing in the irreducible decomposition in general, the complex conjugates of the two irreducible connections arising from $W_4(\alpha_3^+, 1)$ appear in the irreducible decomposition of $W_4(\alpha_3^-, 1)$. In this way, we see that switching the positive and negative braiding for the α-induced connections amounts to taking complex conjugate connections. The same argument also works for E_7 and E_8. This was also observed by Ocneanu [45], but is special to the A-D-E Dynkin diagrams. The decomposition rules for E_7 as in [8, Figure 42] follow from our computations in [14] showing that the principal graph of the subfactor arising from the E_7 connection is D_{10}.

The modular tensor categories corresponding to the Wess–Zumino–Witten model $SU(N)_k$ also have $\mathbb{Z}/N\mathbb{Z}$-grading, and a similar method to the above shows how to handle this issue.

We add a remark on the effect of Assumption 2.2. Even without this Assumption, our Definitions 3.1, 3.3, 3.4, and 3.5 on our new connections make sense. The only problem is that if horizontal graphs are disconnected, we cannot compose two

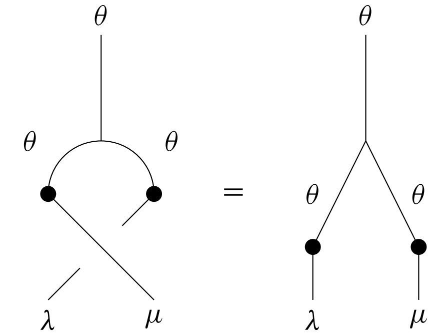

Figure 37. A consequence of Figure 36.

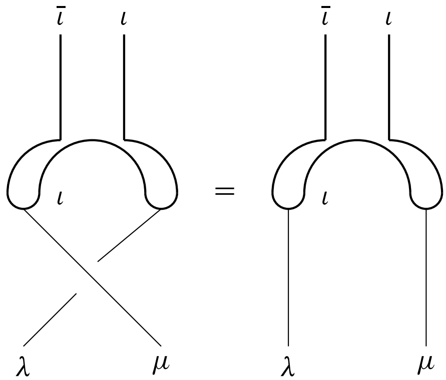

Figure 38. A consequence of Figure 37.

connections in a usual way in Theorem 3.6, and other results such as Theorem 5.2 are not affected. Another way of handling the issue in Assumption 2.2 is to make Δ smaller. For example, if we choose $\lambda = \mu = 2$ in the numbering of irreducible objects for the fusion category $SU(2)_k$ as in Figure 41 and consider only irreducible objects numbered with even integers, then everything in the above sections works fine.

7. Triple sequence of string algebras and another interpretation of the α-induction in terms of bi-unitary connections

Let $*$ be the vertex corresponding to the identity automorphism of N in Δ. We construct a triple sequence $\{A_{jkl}\}_{jkl}$ as in [25, Section 2]. This is a triple sequence version of the standard construction of the double sequence of string algebras in [15, Section 11.3]. A new property we need for compatibility of the identification is the

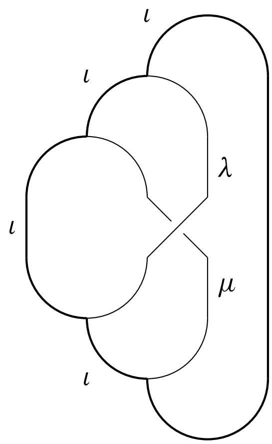

Figure 39. A diagram for the connection $W_4(\alpha_\lambda^+, \mu)$ for $a_1 = a_2 = a_3 = a_4 = \iota$.

intertwining Yang–Baxter equations as in [25, Axiom 7], and we now have this identity as in Figure 25.

For the commuting squares

$$\begin{array}{ccc} A_{2j,2k,2l} & \subset & A_{2j,2k+1,2l} \\ \cap & & \cap \\ A_{2j+1,2k,2l} & \subset & A_{2j+1,2k+1,2l} \end{array},$$

$$\begin{array}{ccc} A_{2j,2k,2l+1} & \subset & A_{2j,2k+1,2l+1} \\ \cap & & \cap \\ A_{2j+1,2k,2l+1} & \subset & A_{2j+1,2k+1,2l+1} \end{array},$$

$$\begin{array}{ccc} A_{2j,2k,2l} & \subset & A_{2j,2k+1,2l} \\ \cap & & \cap \\ A_{2j,2k,2l+1} & \subset & A_{2j,2k+1,2l} \end{array},$$

$$\begin{array}{ccc} A_{2j+1,2k,2l} & \subset & A_{2j+1,2k+1,2l} \\ \cap & & \cap \\ A_{2j+1,2k,2l+1} & \subset & A_{2j+1,2k+1,2l} \end{array},$$

$$\begin{array}{ccc} A_{2j,2k,2l} & \subset & A_{2j+1,2k,2l} \\ \cap & & \cap \\ A_{2j,2k,2l+1} & \subset & A_{2j+1,2k,2l+1} \end{array},$$

$$\begin{array}{ccc} A_{2j,2k+1,2l} & \subset & A_{2j+1,2k+1,2l} \\ \cap & & \cap \\ A_{2j,2k+1,2l+1} & \subset & A_{2j+1,2k+1,2l+1} \end{array},$$

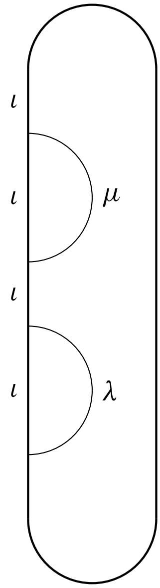

Figure 40. Redrawing of Figure 39 with Lemma 5.1.

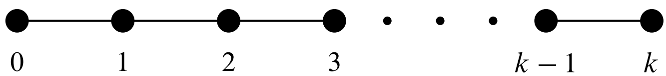

Figure 41. Irreducible objects for the $SU(2)_k$ WZW-model.

we use the connections $W_1(\lambda,\mu)$, $W_4(\alpha^+_\lambda,\mu)$, $W_2(\mu)$, $W_2(\mu)$, $W_3(\lambda)$, and $W_3(\lambda)$, respectively. We then have the following identification between the string algebras and the endomorphism spaces:

$$\begin{aligned}
A_{2j,2k,2l} &= \mathrm{End}((\bar\lambda\lambda)^j(\bar\iota\iota)^l(\mu\bar\mu)^k),\\
A_{2j,2k+1,2l} &= \mathrm{End}((\bar\lambda\lambda)^j(\bar\iota\iota)^l(\mu\bar\mu)^k\mu),\\
A_{2j+1,2k,2l} &= \mathrm{End}(\lambda(\bar\lambda\lambda)^j(\bar\iota\iota)^l(\mu\bar\mu)^k),\\
A_{2j+1,2k+1,2l} &= \mathrm{End}(\lambda(\bar\lambda\lambda)^j(\bar\iota\iota)^l(\mu\bar\mu)^k\mu),\\
A_{2j,2k,2l+1} &= \mathrm{End}((\alpha^+_{\bar\lambda}\alpha^+_\lambda)^j\iota(\bar\iota\iota)^l(\mu\bar\mu)^k),\\
A_{2j,2k+1,2l+1} &= \mathrm{End}((\alpha^+_{\bar\lambda}\alpha^+_\lambda)^j\iota(\bar\iota\iota)^l(\mu\bar\mu)^k\mu),\\
A_{2j+1,2k,2l+1} &= \mathrm{End}(\alpha^+_\lambda(\alpha^+_{\bar\lambda}\alpha^+_\lambda)^j\iota(\bar\iota\iota)^l(\mu\bar\mu)^k),\\
A_{2j+1,2k+1,2l+1} &= \mathrm{End}(\alpha^+_\lambda(\alpha^+_{\bar\lambda}\alpha^+_\lambda)^j\iota(\bar\iota\iota)^l(\mu\bar\mu)^k\mu).
\end{aligned}$$

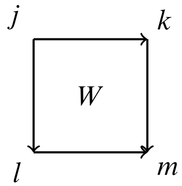

$$= \delta_{kl}\varepsilon + \sqrt{\frac{\mu_k \mu_l}{\mu_j \mu_m}}\delta_{jm}\bar{\varepsilon}$$

Figure 42. A connection on the Dynkin diagram.

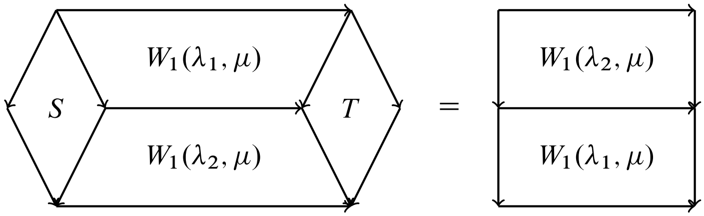

Figure 43. Braiding $\varepsilon^+(\lambda_1, \lambda_2)$.

Note that for inclusions such as $A_{2j,2k,2l} \subset A_{2j,2k,2l+1}$, we use unitary equivalences $\alpha^+_\lambda \iota \cong \iota\lambda$, $\alpha^+_{\bar{\lambda}} \iota \cong \iota\bar{\lambda}$, $\lambda\bar{\iota} \cong \bar{\iota}\alpha^+_\lambda$, and $\bar{\lambda}\bar{\iota} \cong \bar{\iota}\alpha^+_{\bar{\lambda}}$. These are compatible with ways of identification of strings with the connections. (The only nontrivial identification is done with $W_3(\lambda)$, where we use unitary equivalence of $\iota\lambda$ and $\alpha_\lambda\iota$ as in Figure 16.)

By taking unions over k and making the GNS-completions with respect to the compatible trace, we have a commuting square of hyperfinite type II_1 factors as in [25, Assumption 1.1]. We see that our triple sequence of string algebras arise from this commuting square as in [25, Section 3]. See [25, Section 5] for the case of the Dynkin diagrams of type A-D-E.

Our construction of α-induced connections from $N \subset M$ uses information on all the N-M morphisms and their intertwiners. This is also true for Ocneanu's chiral generator picture in Figure 1 in the double triangle algebra. This is theoretically fine, but we would like to have a method to obtain the α-induced connections purely in terms of connections. We discuss such a method at the end of this paper.

In the original setting of the set Δ of irreducible endomorphisms of N, we fix $\mu \in \Delta$ and suppose we have a family of connections $W_1(\lambda, \mu)$ for $\lambda \in \Delta$ and the horizontal top and bottom graphs for all of them are the same finite bipartite graph $\mathcal{G}$. Let $*$ be the vertex of $\mathcal{G}$ corresponding to the identity automorphism in Δ. Our positive braiding gives equivalence of the two composite connections $W_1(\lambda_1, \mu) \cdot W_1(\lambda_2, \mu)$ and $W_2(\lambda_1, \mu) \cdot W_1(\lambda_1, \mu)$. This is given by Figure 43, where S and T give unitary matrices giving vertical gauge choices arising from a positive braiding between λ_1 and λ_2.

Suppose that we have a flat connection W_0 with respect to $*$ (in the sense of [15, Definition 11.16]) with the horizontal top and bottom graphs being finite bipartite graphs $\mathcal{G}$ and $\mathcal{H}$ such that the composition $W_0 \cdot \bar{W}_0$ decomposes into a direct sum of irreducible connections each of which is equivalent to one of $W_1(\lambda, \mu)$. This is a connection version of our setting in Section 2 and our connection W_0 must be of the form $W_2(\mu)$ for some ι.

Construct a double sequence of string algebras $\{B_{kl}\}_{kl}$ as in [15, Section 11.3] from the connection W_0. That is, the commuting square

$$\begin{array}{ccc} B_{2l,2k} & \subset & B_{2l,2k+1} \\ \cap & & \cap \\ B_{2l+1,2k} & \subset & B_{2l+1,2k+1} \end{array}$$

is described with W_0. We further construct a double sequence of string algebras $\{C_{kl}\}_{kl}$ so that

$$\begin{array}{ccc} B_{2l,2k} & \subset & B_{2l,2k+1} \\ \cap & & \cap \\ C_{2l,2k} & \subset & C_{2l,2k+1} \end{array}$$

is described with $W_1(\lambda, \mu)$ and

$$\begin{array}{ccc} C_{2l,2k} & \subset & C_{2l,2k+1} \\ \cap & & \cap \\ C_{2l+1,2k} & \subset & C_{2l+1,2k+1} \end{array}$$

is described with W_0 . Because of the braiding between $W_1(\lambda, \mu)$ and $W_0 \cdot \bar{W}_0$, we have compatibility between

$$\begin{array}{ccc} B_{2l,k} & \subset & B_{2l,k+1} \\ \cap & & \cap \\ C_{2l,k} & \subset & C_{2l,k+1} \\ \cap & & \cap \\ C_{2l+2,k} & \subset & C_{2l+2,k+1} \end{array}$$

and

$$\begin{array}{ccc} B_{2l,k} & \subset & B_{2l,k+1} \\ \cap & & \cap \\ B_{2l+2,k} & \subset & B_{2l+2,k+1} \\ \cap & & \cap \\ C_{2l+2,k} & \subset & C_{2l+2,k+1} \end{array}$$

as in the case of the intertwining Yang–Baxter equation.

Consider an element in $B_{2l+1,k}$. It is embedded into $B_{2l+2,k}$ and then into $C_{2l+2,k}$. It is not a priori clear whether the image in $C_{2l+2,k}$ or not, but actually the image is in

$C_{2l+1,k}$ because we are in the setting of the triple sequence of string algebras introduced in this Section. This gives an embedding of $B_{2l+1,k}$ into $C_{2l+1,k}$. Then, the results in section 3 mean that the connection describing the commuting square

$$\begin{array}{ccc} B_{2l+1,2k} & \subset & B_{2l+1,2k+1} \\ \cap & & \cap \\ C_{2l+1,2k} & \subset & C_{2l+1,2k+1} \end{array}$$

is $W_4(\alpha^+_\lambda, \mu)$.

Acknowledgments. A part of this work was done at Microsoft Station Q at Santa Barbara and University of California, Berkeley. The author thanks for their hospitality.

Funding. This work was partially supported by JST CREST program JPMJCR18T6 and Grants-in-Aid for Scientific Research 19H00640 and 19K21832.

References

[1] M. Asaeda and U. Haagerup, Exotic subfactors of finite depth with Jones indices $(5+\sqrt{13})/2$ and $(5+\sqrt{17})/2$. *Comm. Math. Phys.* **202** (1999), no. 1, 1–63 Zbl 1014.46042 MR 1686551

[2] F. A. Bais and J. K. Slingerland, Condensate induced transitions between topologically ordered phases. *Phys. Rev. B* **79** (2009), article no. 045316, 27 pp.

[3] M. Bischoff, Y. Kawahigashi, R. Longo, and K.-H. Rehren, *Tensor categories and endomorphisms of von Neumann algebras—with applications to quantum field theory*. SpringerBriefs Math. Phys. 3, Springer, Cham, 2015 Zbl 1328.46047 MR 3308880

[4] J. Böckenhauer and D. E. Evans, Modular invariants, graphs and α-induction for nets of subfactors. I. *Comm. Math. Phys.* **197** (1998), no. 2, 361–386 Zbl 0924.46047 MR 1652746

[5] J. Böckenhauer and D. E. Evans, Modular invariants, graphs and α-induction for nets of subfactors. II. *Comm. Math. Phys.* **200** (1999), no. 1, 57–103 Zbl 1151.46316 MR 1671970

[6] J. Böckenhauer and D. E. Evans, Modular invariants, graphs and α-induction for nets of subfactors. III. *Comm. Math. Phys.* **205** (1999), no. 1, 183–228 Zbl 0949.46030 MR 1706884

[7] J. Böckenhauer, D. E. Evans, and Y. Kawahigashi, On α-induction, chiral generators and modular invariants for subfactors. *Comm. Math. Phys.* **208** (1999), no. 2, 429–487 Zbl 0948.46048 MR 1729094

[8] J. Böckenhauer, D. E. Evans, and Y. Kawahigashi, Chiral structure of modular invariants for subfactors. *Comm. Math. Phys.* **210** (2000), no. 3, 733–784 Zbl 0988.46047 MR 1777347

[9] N. Bultinck, M. Mariën, D. J. Williamson, M. B. Şahinoğlu, J. Haegeman, and F. Verstraete, Anyons and matrix product operator algebras. *Ann. Physics* **378** (2017), 183–233 Zbl 1367.81084 MR 3614057

[10] D. Copeland and C. Edie-Michell, Cell systems for $\overline{\mathrm{rep}(u_q(\mathfrak{sl}_n))}$ module categories. [v1] 2023, [v2] 2023, arXiv:2301.13172v2

[11] P. Das, M. Ghosh, S. Ghosh, and C. Jones, Unitary connections on Bratteli diagrams. [v1] 2022, [v2] 2022, arXiv:2211.03822v2

[12] P. Di Francesco, P. Mathieu, and D. Sénéchal, *Conformal field theory*. Grad. Texts Contemp. Phys., Springer, New York, 1997 Zbl 0869.53052 MR 1424041

[13] P. Etingof, S. Gelaki, D. Nikshych, and V. Ostrik, *Tensor categories*. Math. Surveys Monogr. 205, American Mathematical Society, Providence, RI, 2015 Zbl 1365.18001 MR 3242743

[14] D. E. Evans and Y. Kawahigashi, The E_7 commuting squares produce D_{10} as principal graph. *Publ. Res. Inst. Math. Sci.* **30** (1994), no. 1, 151–166 Zbl 0814.46054 MR 1266388

[15] D. E. Evans and Y. Kawahigashi, *Quantum symmetries on operator algebras*. Oxford Math. Monogr., The Clarendon Press, Oxford University Press, New York, 1998 Zbl 0924.46054 MR 1642584

[16] K. Fredenhagen, K.-H. Rehren, and B. Schroer, Superselection sectors with braid group statistics and exchange algebras. I. General theory. *Comm. Math. Phys.* **125** (1989), no. 2, 201–226 Zbl 0682.46051 MR 1016869

[17] K. Fredenhagen, K.-H. Rehren, and B. Schroer, Superselection sectors with braid group statistics and exchange algebras. II. Geometric aspects and conformal covariance. *Rev. Math. Phys.* (1992), no. Special Issue, 113–157 Zbl 0774.46041 MR 1199171

[18] F. M. Goodman, P. de la Harpe, and V. F. R. Jones, *Coxeter graphs and towers of algebras*. Math. Sci. Res. Inst. Publ. 14, Springer, New York, 1989 Zbl 0698.46050 MR 0999799

[19] S. Goto, On the fusion algebras of bimodules arising from Goodman–de la Harpe–Jones subfactors. *J. Math. Sci. Univ. Tokyo* **19** (2012), no. 4, 409–506 Zbl 1303.46050 MR 3086735

[20] S. Hollands, Anyonic chains—α-induction—CFT—defects—subfactors. *Comm. Math. Phys.* **399** (2023), no. 3, 1549–1621 Zbl 1522.81505 MR 4580529

[21] M. Izumi, Subalgebras of infinite C^*-algebras with finite Watatani indices. II. Cuntz–Krieger algebras. *Duke Math. J.* **91** (1998), no. 3, 409–461 Zbl 0949.46023 MR 1604162

[22] M. Izumi, The structure of sectors associated with Longo–Rehren inclusions. I. General theory. *Comm. Math. Phys.* **213** (2000), no. 1, 127–179 Zbl 1032.46529 MR 1782145

[23] V. F. R. Jones, Index for subfactors. *Invent. Math.* **72** (1983), no. 1, 1–25 Zbl 0508.46040 MR 0696688

[24] V. F. R. Jones, A polynomial invariant for knots via von Neumann algebras. *Bull. Amer. Math. Soc. (N.S.)* **12** (1985), no. 1, 103–111 Zbl 0564.57006 MR 0766964

[25] Y. Kawahigashi, Classification of paragroup actions in subfactors. *Publ. Res. Inst. Math. Sci.* **31** (1995), no. 3, 481–517 Zbl 0837.46046 MR 1355948

[26] Y. Kawahigashi, On flatness of Ocneanu's connections on the Dynkin diagrams and classification of subfactors. *J. Funct. Anal.* **127** (1995), no. 1, 63–107 Zbl 0829.46048 MR 1308617

[27] Y. Kawahigashi, Conformal field theory, tensor categories and operator algebras. *J. Phys. A* **48** (2015), no. 30, article no. 303001, 57 pp. Zbl 1328.81194 MR 3367967

[28] Y. Kawahigashi, Conformal field theory, vertex operator algebras and operator algebras. In *Proceedings of the International Congress of Mathematicians—Rio de Janeiro 2018. Vol. III. Invited lectures*, pp. 2597–2616, World Scientific, Hackensack, NJ, 2018 Zbl 1447.81179 MR 3966864

[29] Y. Kawahigashi, A remark on matrix product operator algebras, anyons and subfactors. *Lett. Math. Phys.* **110** (2020), no. 6, 1113–1122 Zbl 1470.46089 MR 4109480

[30] Y. Kawahigashi, Two-dimensional topological order and operator algebras. *Internat. J. Modern Phys. B* **35** (2021), no. 8, article no. 2130003, 16 pp. Zbl 1462.81001 MR 4272039

[31] Y. Kawahigashi, A characterization of a finite-dimensional commuting square producing a subfactor of finite depth. *Int. Math. Res. Not. IMRN* **2023** (2023), no. 10, 8419–8433 Zbl 07690532 MR 4589077

[32] Y. Kawahigashi, Projector matrix product operators, anyons and higher relative commutants of subfactors. *Math. Ann.* **387** (2023), no. 3-4, 2157–2172 Zbl 07758187 MR 4657446

[33] Y. Kawahigashi and R. Longo, Classification of local conformal nets. Case $c < 1$. *Ann. of Math. (2)* **160** (2004), no. 2, 493–522 Zbl 1083.46038 MR 2123931

[34] Y. Kawahigashi, R. Longo, and M. Müger, Multi-interval subfactors and modularity of representations in conformal field theory. *Comm. Math. Phys.* **219** (2001), no. 3, 631–669 Zbl 1016.81031 MR 1838752

[35] Y. Kawahigashi, R. Longo, U. Pennig, and K.-H. Rehren, The classification of non-local chiral CFT with $c < 1$. *Comm. Math. Phys.* **271** (2007), no. 2, 375–385 Zbl 1131.81031 MR 2287908

[36] L. Kong, Anyon condensation and tensor categories. *Nuclear Phys. B* **886** (2014), 436–482 Zbl 1325.81156 MR 3246855

[37] R. Longo, Index of subfactors and statistics of quantum fields. I. *Comm. Math. Phys.* **126** (1989), no. 2, 217–247 Zbl 0682.46045 MR 1027496

[38] R. Longo, Index of subfactors and statistics of quantum fields. II. Correspondences, braid group statistics and Jones polynomial. *Comm. Math. Phys.* **130** (1990), no. 2, 285–309 Zbl 0705.46038 MR 1059320

[39] R. Longo, A duality for Hopf algebras and for subfactors. I. *Comm. Math. Phys.* **159** (1994), no. 1, 133–150 Zbl 0802.46075 MR 1257245

[40] R. Longo and K.-H. Rehren, Nets of subfactors. *Rev. Math. Phys.* **7** (1995), no. 4, 567–597 Zbl 0836.46055 MR 1332979

[41] L. Lootens, J. Fuchs, J. Haegeman, C. Schweigert, and F. Verstraete, Matrix product operator symmetries and intertwiners in string-nets with domain walls. *SciPost Phys.* **10** (2021), no. 3, article no. 053, 42 pp. MR 4237747

[42] T. Masuda, An analogue of Longo's canonical endomorphism for bimodule theory and its application to asymptotic inclusions. *Internat. J. Math.* **8** (1997), no. 2, 249–265 Zbl 0909.46044 MR 1442437

[43] A. Ocneanu, Quantized groups, string algebras and Galois theory for algebras. In *Operator algebras and applications, Vol. 2*, pp. 119–172, London Math. Soc. Lecture Note Ser. 136, Cambridge University Press, Cambridge, 1988 Zbl 0696.46048 MR 0996454

[44] A. Ocneanu, *Quantum symmetry, differential geometry of finite graphs and classification of subfactors*. University of Tokyo Seminary Notes 45, University of Tokyo, Japan, 1991

[45] A. Ocneanu, Paths on coxeter diagrams: from Platonic solids and singularities to minimal models and subfactors. In *Lectures on operator theory*, pp. 243–323, Fields Inst. Monogr., American Mathematical Society, Providence, RI, 2000

[46] S. Popa, Maximal injective subalgebras in factors associated with free groups. *Adv. in Math.* **50** (1983), no. 1, 27–48 Zbl 0545.46041 MR 0720738

[47] S. Popa, Classification of amenable subfactors of type II. *Acta Math.* **172** (1994), no. 2, 163–255 Zbl 0853.46059 MR 1278111

[48] N. Sato, Constructing a nondegenerate commuting square from equivalent systems of bimodules. *Internat. Math. Res. Notices* (1997), no. 19, 967–981 Zbl 0934.46060 MR 1488347

[49] J. K. Schou, *Commuting squares and index for subfactors*. Ph.D. thesis, Odense University, Denmark, 1990

[50] A. Wassermann, Operator algebras and conformal field theory. III. Fusion of positive energy representations of LSU(N) using bounded operators. *Invent. Math.* **133** (1998), no. 3, 467–538 Zbl 0944.46059 MR 1645078

[51] F. Xu, New braided endomorphisms from conformal inclusions. *Comm. Math. Phys.* **192** (1998), no. 2, 349–403 Zbl 0908.46044 MR 1617550

[52] F. Xu, Jones–Wassermann subfactors for disconnected intervals. *Commun. Contemp. Math.* **2** (2000), no. 3, 307–347 Zbl 0966.46043 MR 1776984

Received 20 February 2023.

Yasuyuki Kawahigashi
Graduate School of Mathematical Sciences, The University of Tokyo, 3-8-1 Komaba, Tokyo 153-8914, Japan; yasuyuki@ms.u-tokyo.ac.jp